JOURNAL OF AGRICULTURAL AND FOOD CHEMISTRY

Structural and Molecular Basis of Starch Viscosity in Hexaploid Wheat

J.-P. RAL,[†] C. R. CAVANAGH,[†] O. LARROQUE,[†] A. REGINA,[†] AND M. K. MORELL*,[†,‡]

Food Futures National Research Flagship, Commonwealth Scientific and Industrial Research Organization, P.O. Box 93, North Ryde 1670, NSW, Australia, and Plant Industry, Commonwealth Scientific and Industrial Research Organization, GPO Box 1600, Canberra ACT 2601, Australia

Wheat starch is considered to have a low paste viscosity relative to other starches. Consequently, wheat starch is not preferred for many applications as compared to other high paste viscosity starches. Increasing the viscosity of wheat starch is expected to increase the functionality of a range of wheat flour-based products in which the texture is an important aspect of consumer acceptance (e.g., pasta, and instant and yellow alkaline noodles). To understand the molecular basis of starch viscosity, we have undertaken a comprehensive structural and rheological analysis of starches from a genetically diverse set of wheat genotypes, which revealed significant variation in starch traits including starch granule protein content, starch-associated lipid content and composition, phosphate content, and the structures of the amylose and amylopectin fractions. Statistical analysis highlighted the association between amylopectin chains of 18−25 glucose residues and starch pasting properties. Principal component analysis also identified an association between monoesterified phosphate and starch pasting properties in wheat despite the low starch−phosphate level in wheat as compared to tuber starches. We also found a strong negative correlation between the phosphate ester content and the starch content in flour. Previously observed associations between internal starch granule fatty acids and the swelling peak time and pasting temperature have been confirmed. This study has highlighted a range of parameters associated with increased starch viscosity that could be used in prebreeding/breeding programs to modify wheat starch pasting properties.

KEYWORDS: Starch; viscosity; wheat; structure; phosphate; fatty acids; statistical analysis; DSC; RVA

INTRODUCTION

Starch is the major carbohydrate reserve in plants, and it is also the major energy-providing component in human diets. The importance of starch functionality for end product quality has gained increased recognition recently. Starch attributes contribute to many aspects of textural properties and are the basis of more than 600 industrial applications (e.g., gelling agent, bulking agent, water retention agent, and adhesive).

Starch consists of α-1,4-linked glucose residues, which are branched in the α-1,6-position. It is composed of two distinct insoluble fractions, the amylopectin and the amylose. Amylopectin is the major fraction of the starch granule, and it is made of large molecules ranging in size (∼10000−100000 glucosyl residues) and contains around 5% α-1,6-branches. Amylose, on the other hand, is the minor fraction of the starch granule and represents 20−30% of the polysaccharide content. Amylose molecules range in size between 100 and 1000 glucosyl residues with less than 1% α-1,6-branches (for a review, see ref *1*).

Since the 1920s and the first studies of the pasting properties of wheat starch (*2*), viscosity has remained an important focus for food scientists. Recently, chemically modified starches such as acetylated, esterified, and etherified starches have been incorporated in a wide range of prepared foods such as snacks, cakes, and most commonly in bread. Chemically modified starches have also been produced to modify the functionality of native starches including their viscosity. However, these chemically modified starches have limitations in complex systems such as wheat flour-based products. Understanding the structural and molecular basis of wheat starch viscosity will allow selection for modified starch in planta tailored to end use products.

Amylose influences both the rheological and the viscoelastic characteristics, including gelatinization and retrogradation (*3*). Oda et al. (*4*) demonstrated that reduced amylose content leads to a reduction in both the gel temperature and the temperature at the maximum viscosity. Furthermore, morphological characteristics such as shape and size of the starch granule and their innate crystalline structure could be an explanation for this

* To whom correspondence should be addressed. Tel: +61-2-6246 5074. Fax: +61-2-62465345. E-mail: Matthew.Morell@csiro.au.
[†] Food Futures National Research Flagship.
[‡] Plant Industry.

10.1021/jf800124f CCC: $40.75
Published on Web 05/07/2008

variability (*5*). Lipids may also have an impact on the rheological properties of starch granules (*6*). Morrisson et al. (*7*) suggested that, even at a very low level, the presence of starch lipids affects the visco-properties of starch granules. Potato starch displays a much higher viscosity than cereals, particularly wheat. There are two hypotheses regarding the high viscosity of potato. First, potato starch contains a higher content of phosphate groups as compared with wheat, and a link between these phosphate groups and the swelling properties has been made (*6*). Second, it has been suggested that the structural differences of amylopectin between cereals and potato are associated with a variation in their crystallinity (*8*).

Many methods have been developed to characterize starch rheological properties from various plant sources such as potato, rice, and cassava (*9, 10*) or to study the influence of a particular character on the viscosity. Studies in maize and potato starch have been conducted to define new products with high potential for industrial purposes (*11–13*). Starch properties of commercial hexaploid wheat do not display large variation.

A multitude of analyses have been performed on the effect of lipids and amylose content on the starch rheological properties (for a review, see ref *14*). However, it would be useful to consider most of the physicochemical properties of starch and relate these to the various aspects of the starch rheological properties. In addition, actual measurements of the gelatinization and viscosity are time and material consuming. Defining a reliable correlation between physical or molecular properties and viscosity will enable high throughput screening of wheat germplasm.

In this study, a selection of nine genotypes with similar amylopectin/amylose ratios have been selected for their particular physicochemical properties. Some cultivars are empirically known to be relevant for baking and noodle making (e.g., Chara). Some are known to be good for Asian-steamed bread (e.g., Baxter) and others for their sponge and dough bread baking properties (e.g., AC-Barrie). We decided to add two control lines with drastic amylopectin/amylose ratios. Because of their extreme properties, these controls will serve as references but will not be a part of the statistical survey. The identification of wheat varieties with altered starch properties will pave the way for new end products utilizing wheat starch. The aim of this study is to survey the variation in starch properties and their structural characteristics in relation to their functional characteristics in bread wheat.

MATERIALS AND METHODS

Isoamylase, pullulanase, and β-amylase from *B. cereus* were obtained from Megazyme International Ireland Limited. CL2B Sepharose column was obtained from Amersham Pharmacia Biotech. A starch assay kit was obtained from Roche (Germany).

Plant Material. Nine wheat cultivars and two mutant lines were selected to represent a diverse set of Australian and international cultivars. The cultivars were selected after genetic distance measures, and the measures were based on 360 Diversity Array Technology (DArT) markers (*15*) analyzed on 180 international wheat cultivars. In addition, their geographic origin and end product uses were assessed to incorporate maximum trait diversity (Cavanagh, C. R. Unpublished data). These lines are to be utilized in mapping populations and therefore are of particular interest to this group.

Two mutant lines have been included as controls. These two mutant lines have extreme amylose phenotypes: The first (EH6) is a triple null mutant at the GBSSI loci and displays a nonamylose (waxy) phenotype, and the second is a high amylose mutant (Yamamori). Details of all lines are included as references. All cultivars were grown at the same time and under controlled conditions in a glasshouse. The mutant lines were grown under quarantine conditions at the same time.

Starch Characterization. *Starch Extraction.* Starch was extracted from ground grain by hand washing with deionized water (*16*). A 5 mL aliquot of each starch slurry was frozen for particle size analysis. The remainder was freeze-dried in an FTS Freeze Drier (model no. FD-3-55D-MP).

Granule Size Distribution. The granule size distribution of the thawed starch slurries was determined using a laser diffraction particle size analyzer (model 2600c Droplet and Particle Sizer, Malvern Instruments, Malvern, United Kingdom). The volume percentage of starch granules less than 10 μm in diameter (B-granules) was the measurement used in this study. Freeze-dried starch was used for the remaining methods.

Swelling Test. The 40 mg swelling test (*17*) was used to determine the starch swelling power. This test measured the uptake of water during the gelatinization of starch. The gain in weight of the starch gel, following gelatinization at 92.5 °C, was converted to a swelling power.

Differential Scanning Calorimetry (DSC). DSC was performed using a Seiko 22C DSC (*18*). Starch and water were premixed in a ratio of 1:2 (dry basis), and then, approximately 15 mg was placed in a DSC pan, hermetically sealed, and placed in the DSC. The reference was an empty pan, and the heating profile was 10 °C for 2 min, 10−140 at 10 °C/min, and 140 °C for 2 min. Two endotherm peaks occurred. The first, around 60 °C, represented the breakdown of the crystalline structure during starch gelatinization. The second, around 110 °C, represented the amylose−lipid dissociation (*19*). The onset, peak, and final temperatures of each endotherm were measured, as was the ΔH (enthalpy) in mJ/mg.

Pasting Properties. Starch pasting properties were analyzed using an rapid visco analyzer (RVA type 4) (Newport Scientific, Sydney, Australia). A 9% starch sample suspension was equilibrated at 50 °C for 2 min, heated to 95 °C over 6 min, maintained at temperature for 4 min, cooled to 50 °C over 4 min, and finally maintained at 50 °C for 5 min. A constant rotating speed of the paddle (160 rpm) was used throughout the analysis.

Separation of Starch Polysaccharide by Gel Permeation Chromatography. A total of 1−2.5 mg of starch dissolved in 500 μL of 10 mM NaOH was applied to a Sepharose CL2B column [0.5 cm (i.d.) × 65 cm] equilibrated in 10 mM NaOH. Fractions of 250−300 μL were collected at a rate of 1 fraction/1.5 min. Glucans in each fraction were detected through the iodine−polysaccharide interaction.

Amylose Content. The amylose content was measured using a small scale (1 mg of starch) iodine adsorption method (*20*). A microtiter plate reader was used to compare the samples to standards, and on the basis of a calibration curve, the percent amylose content was estimated. The absorbance was read at 620 nm on three samples per replicate analysis and averaged.

Fluorophore-Assisted Carbohydrate Electrophoresis Chain Length Distribution. The chain length distribution of wheat endosperm starch was analyzed as described by Morell et al. (*21*) using a P/ACE 5510 capillary electrophoresis system (Beckman) with argon-LIF detection. This analysis has been realized three times.

Starch Lipid Determination. Nonstarch lipids were washed from 150 mg of dry starch following the cold water-saturated butan-1-ol extraction method (*22*). This step removes any lipids that may attach to the outside of the starch granules. Starch lipids were extracted from the starch following the hot propan-1-ol water (3:1) method (*23*). Dry samples were methylated, and the starch lipids determination was performed by gas chromotography (GC) analysis.

Starch Proteins Quantification. Proteins associated with starch granules were measured via a nitrogen quantification using mass spectrometry analysis.

Phosphate Quantification. The total phosphate content in starch was determined using an adapted Malachite green method (*24*). Ten milligrams of dry starch was solubilized in 500 μL of 10% DMSO solution and boiled for 10 min. Two hundred microliters of suspension was then mixed with 200 μL of Clark and Lub Buffer (0.054 M KCl and 0.145 M HCl), 120 μL of H_2O, 80 μL of 4 M HCl, and 200 μL of Malachite green solution 3:1 [0.2% Malachite green solution; 10% $(NH_4)_6Mo_7O_{24}(4H_20)$ solution on 4 M HCl]. A spectrophotometer was used to compare the samples to standards, and on the basis of a calibration curve, the phosphate content was estimated. The optical

Table 1. Molecular Composition and Wheat Starch Characterization[a]

	starch content (% in flour)	internal fatty acid (%)	internal protein (%)	amylose content (%)	starch λ_{max} (nm)	granule size: average size (μm)	granule size: B-granule (%)	Glc6P content (μg mg starch^{-1})
Yamamori	66.02 ± 1.23	1.02 ± 0.01	0.51 ± 0.02	42.18 ± 4.8	604 ± 1.87	16.27 ± 0.89	24.18 ± 0.84	13.78 ± 0.51
EH6	64.37 ± 3.46	0.44 ± 0.05	0.09 ± 0.01	3.21 ± 1.1	530 ± 3.50	17.12 ± 0.7	32.77 ± 1.01	7.02 ± 0.89
VolcaniDD1	62.27 ± 0.6	0.73 ± 0.02	0.17 ± 0.02	24.12 ± 1	591 ± 3.70	17.86 ± 0.89	29.28 ± 0.99	18.17 ± 0.69
Pastor	64.49 ± 1.34	0.84 ± 0.02	0.12 ± 0.01	28.63 ± 0.5	591 ± 3.67	19.36 ± 0.81	22.56 ± 0.96	14.12 ± 1.47
AC-Barrie	65.82 ± 2.91	0.69 ± 0.03	0.11 ± 0.01	34.25 ± 1.9	592 ± 3.61	15.25 ± 1	34.03 ± 1.05	16.31 ± 1.7
Alsen	65.6 ± 1.96	0.79 ± 0.04	0.14 ± 0.01	37.66 ± 1.3	588 ± 2.86	12.94 ± 1.14	41.92 ± 1.2	8.85 ± 1.8
Westonia	70.59 ± 0.33	0.55 ± 0.05	0.11 ± 0.01	20.15 ± 0.2	590 ± 2.29	19.31 ± 0.85	26.43 ± 0.93	11.87 ± 0.88
Xiaoyan54	60.83 ± 2.4	1.26 ± 0.01	0.14 ± 0.01	33.15 ± 4.4	603 ± 2.55	17.08 ± 0.81	23.57 ± 0.97	24.77 ± 1.17
Yitpi	69.14 ± 2.81	0.7 ± 0.03	0.1 ± 0.01	24.79 ± 2.8	591 ± 0.83	18.85 ± 0.87	27.88 ± 0.99	17.54 ± 1.2
Chara	75.63 ± 1.96	0.75 ± 0.05	0.14 ± 0.01	22.28 ± 0.3	585 ± 1.79	15.38 ± 1.06	34.55 ± 1.19	5.67 ± 0.59
Baxter	71.72 ± 2.53	0.55 ± 0.05	0.1 ± 0.01	28.41 ± 5.4	601 ± 1.79	17.1 ± 0.91	30.56 ± 1	9.79 ± 0.43

[a] Results displayed are the means of three independent assays.

density was read at 660 nm on three samples per replicate analysis, and results were averaged.

Glucose-6-phosphate (Glc6P) was estimated by an adapted amyloglucosidase assay using the starch assay kit from Roche (Germany). Glc6P dehydrogenase was used specifically in this assay.

Statistical Analysis. Correlation analysis between starch pasting properties and structural components was carried out in Genstat (8th ed.) using the correlation function. Isoamylase and β-amylase chain length (CL) distributions were analyzed independently to determine those chain lengths with higher standard deviations. In addition, those highly correlated chain lengths were grouped together (e.g., CL_18 to 25) and analyzed as a single combined trait to reduce the number of tests to be conducted. Principal component analysis (PCA) was conducted in the statistical software package R (R Development Core Team 2006) using the "prcomp" based on the correlation matrix.

RESULTS AND DISCUSSION

Starch Molecular Properties. The amount of starch present in seed from the cultivars was estimated (**Table 1**). After estimation, the genotypes were classified into three categories: (i) VolcaniDD1, Pastor, and Xiaoyan54, which display a low percentage of starch (below 65%); (ii) a group ranging from 65 to 70% (AC-Barrie, Alsen, and Yitpi); and (iii) a group with more than 70% starch (Westonia, Chara, and Baxter).

The role of starch-associated phosphate has been demonstrated to be relevant for starch viscosity in potato (*25*). Glc6P, which represents almost 80% of the starch-associated phosphate monoesters, was estimated via an enzymatic assay (**Table 1**). The Glc6P content varied from 5.67 to 24.77 μg per mg starch. On the basis of the Glc6P, the genotypes could be classified into three groups: (i) low Glc6P (Alsen, Chara, and Baxter), (ii) medium Glc6P content (Westonia, Pastor, and AC-Barrie), and (iii) high Glc6P content (Yitpi, VolcaniDD1, and Xiaoyan54). It is interesting to note that Xiaoyan54 is known to be affected in the phosphate assimilation pathway (*26*) and showed the highest content of phosphate monoesters.

Following the starch extraction, the mean diameter and the proportion of B-granules from each genotype were measured by a laser diffraction particle size analyzer (**Table 1**). There was a large variation in starch morphology. Alsen had the highest proportion of B-granules and the lowest average granule size while Pastor and Westonia displayed the opposite phenotype.

The protein content was low among the starch samples. VolcaniDD1, known to be a high protein content line, had the highest starch-associated protein amount (0.17%).

We identified a large variation in the amount of starch-associated lipids between the genotypes. The values ranged from 0.55 to 1.26% of dried mass, with Xiaoyan54 having the highest content of the studied genotypes. Yamamori and EH6 displayed 1.02 and 0.44%, respectively. Internal wheat starch lipids are known to represent 1% of the granular weight. However, lipids significantly affect the swelling properties of wheat starch (*7*). Therefore, the decision was taken to perform further analysis of these starch-associated lipids by a specific determination of fatty acids using the GC technique (*22*).

Starch Lipid Determination. The GC technique allowed us to detect and quantify 13 fatty acids from wheat starch (see **Figure 1**). Within these 13 fatty acids, three represented more than 95% of the starch lipid composition (linoleic, palmitic, and oleic acid), while linolenic and stearic acid were the next largest proportion of the starch lipid (**Figure 1A**). Xiaoyan54 was the genotype with the highest proportion of fatty acids. We noticed that VolcaniDD1 and Alsen display a high relative amount of oleic acid and stearic acid, respectively. On the contrary, Westonia and Baxter had the lower total starch fatty acid amount and showed the lowest amount of each individual fatty acid.

Structural Properties of Starch. Starch glucose chains may interact with iodine molecules to form a complex. In the presence of iodine molecules, glucose chains adopt a helicoidal configuration where the iodine is located; the longer the glucose chain is, the higher the iodine incorporation will be (*27*). These data are shown in **Table 1**. All genotypes displayed an average λ_{max} of around 590 nm with the exception of Baxter and Xiaoyan54, for which their wavelengths were more than 600 nm, and Chara, with a slightly lower value of 585 nm. The higher λ_{max} strongly suggested an increase in amylopectin long chains or an increase of amylose content.

The amylose content determined by iodometric estimation was confirmed by estimating the amylose/amylopectin ratio after separation on a CL2B gel permeation chromatography (**Table 1**). With the exception of the two control lines (EH6 and Yamamori) displaying 3.28 and 42% amylose, respectively, the genotypes contain between 20 and 37% amylose with Westonia displaying the lowest amylose percentage and Alsen the highest.

To investigate whether structural modifications occurred in the amylopectin molecule, amylopectin from all genotypes was digested by an isoamylase/pullulanase mix to complete enzymatic debranching. The chain length distribution was determined by FACE (fluorescence-assisted capillary electrophoresis) after coupling with APTS (**Figure 2**). All wheat varieties showed a typical polymodal distribution, observed throughout the plant kingdom, with a maximum at the degree of polymerization (DP) equal to 11. Chara showed a phenotype with a smooth distribution including a slight decrease at the DP = 11% age. However, the profile exhibited by Alsen was particularly different. Chains of DP = 10−17 were strongly increased while

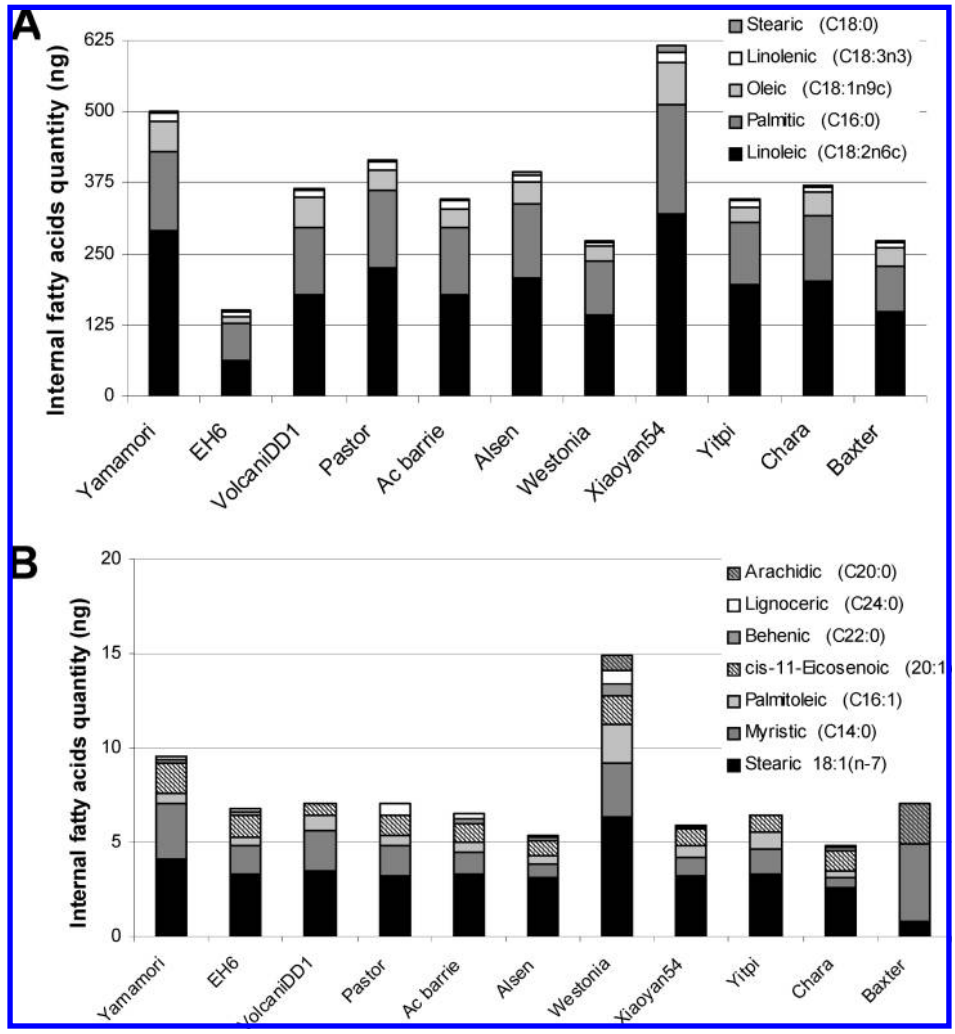

Figure 1. Internal fatty acid composition of wheat starches. The figure displays the five main internal fatty acids present in wheat starch: Major fatty acids associated with starch granules are displayed in panel **A**. The minor fatty acids are displayed in panel **B**. The internal fatty acid content is expressed in ng.

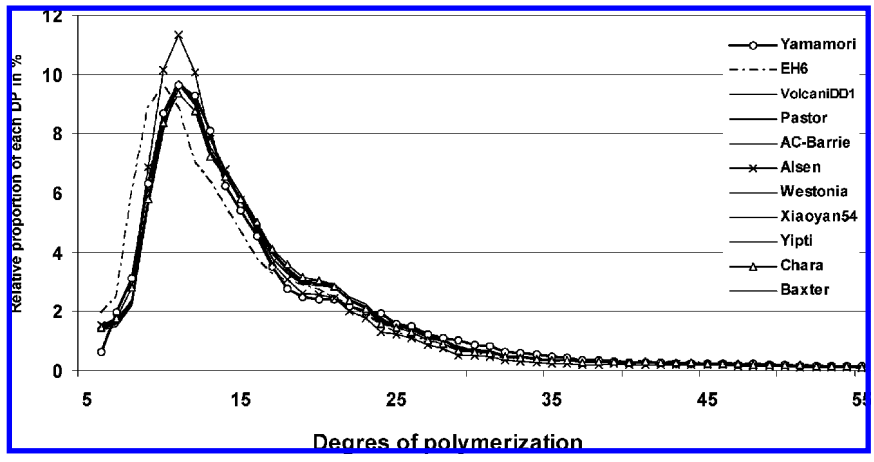

Figure 2. Chain length distribution differences of amylopectin from wheat genotypes. Chain length distributions obtained after isoamylase-mediated enzymatic disbranching through capillary electrophoresis of APTS-labeled fluorescent glucans. The profiles with the more significant modification are highlighted.

chains of DP = 6−9 were reduced. We could also observe a shift in the maximum DP from 11 to 13.

To complete our structural characterization, a β-amylolysis analysis followed by isoamylase debranching and chain length distribution analysis was performed (**Figure 3**). Using this exoenzyme, the external chains are digested while the internal chains are degraded until their first branch point and the amylopectin backbone are revealed. The differential profiles corresponding to the wheat varieties and mutants are shown in **Figure 3**. Baxter, Alsen, and Westonia displayed a slight decrease in DP < 10, while Yitpi showed a low amount of chains from DP 11 to 20. For average long DP between (20 <

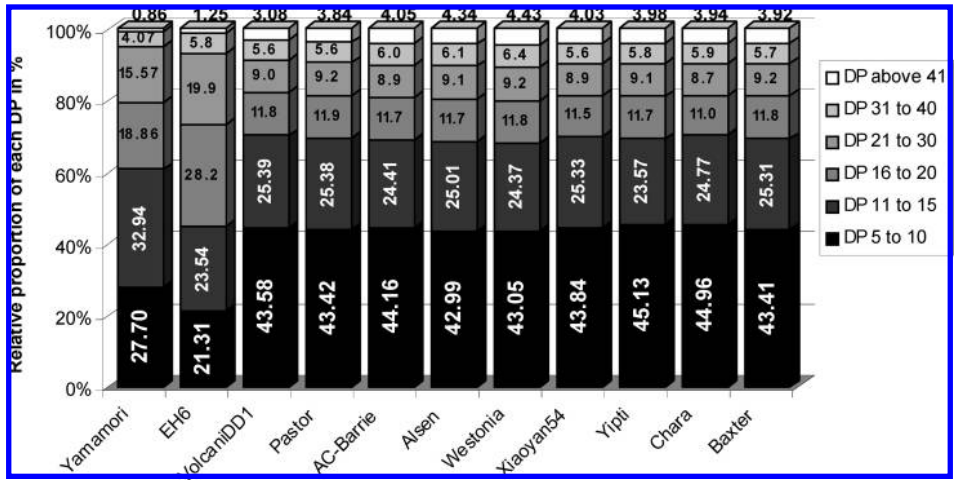

Figure 3. β-Amylolysis chain length distribution differences of amylopectin from wheat genotypes. Chain length distributions obtained after β-amylase treatment directly followed by isoamylase-mediated enzymatic disbranching through capillary electrophoresis of APTS-labeled fluorescent glucans. The main value of each chains included in the graphic is the average result of three independent experiments.

Table 2. Gelatinization Properties of Wheat Starches[a]

		gelatinization				amylose−lipids dissociation			
	SI	T_o (°C)	T_p (°C)	T_c (°C)	ΔH (J/g)	T_o (°C)	T_p (°C)	T_c (°C)	ΔH (J/g)
Yamamori	7.01 ± 0.49	53.53 ± 0.4	58.23 ± 1.6	63.47 ± 0.8	0.91 ± 0.0	86.75 ± 0.7	96.64 ± 0.1	105.70 ± 0.0	1.39 ± 0.1
EH6	1.92 ± 0.6	60.96 ± 0.3	68.44 ± 0.1	88.46 ± 1.6	5.17 ± 0.2				
VolcaniDD1	11.99 ± 0.44	61 ± 0.1	65.3 ± 0.1	70.80 ± 0.0	4.85 ± 0.2	100.15 ± 0.1	105.03 ± 0.1	114.67 ± 0.1	0.77 ± 0.0
Pastor	12.91 ± 0.25	60.42 ± 0.0	64.12 ± 0.2	69.19 ± 0.3	5.13 ± 0.4	99.80 ± 1.4	105.03 ± 0.9	114.13 ± 0.8	0.88 ± 0.1
AC-Barrie	11.66 ± 0.40	60.58 ± 0.5	64 ± 0.2	69.06 ± 0.3	4.81 ± 0.2	100.25 ± 0.6	104.93 ± 1.0	114.67 ± 0.0	0.58 ± 0.1
Alsen	15.91 ± 0.65	60.91 ± 0.1	65.39 ± 0.1	72.36 ± 0.1	5.40 ± 0.5	97.13 ± 0.6	108.89 ± 0.0	114.25 ± 0.0	0.99 ± 0.0
Westonia	14.31 ± 0.56	61.05 ± 0.3	64.80 ± 0.3	70.19 ± 0.1	5.36 ± 0.1	97.36 ± 0.2	103.62 ± 0.0	113.51 ± 0.0	0.74 ± 0.0
Xiaoyan54	12.92 ± 0.36	61.03 ± 0.1	64.74 ± 0.3	70.32 ± 0.6	5.61 ± 0.2	97.92 ± 0.0	104.66 ± 0.5	110.98 ± 0.2	1.11 ± 0.0
Yipti	15.09 ± 0.6	60.11 ± 0.2	63.92 ± 0.1	69.19 ± 0.4	5.48 ± 0.1	97.84 ± 0.6	105.1 ± 0.0	113.68 ± 0.2	0.88 ± 0.0
Chara	12.94 ± 0.74	62.52 ± 0.0	66.47 ± 0.0	72.01 ± 0.1	5.90 ± 0.1	93.17 ± 4.4	102.95 ± 1.2	113.64 ± 0.1	0.81 ± 0.0
Baxter	11.15 ± 0.21	61.05 ± 0.2	65.6 ± 0.1	71.25 ± 0.3	5.11 ± 0.3	97.55 ± 0.3	103.97 ± 0.1	113.53 ± 0.0	0.86 ± 0.0

[a] SI represents the SI produced at 90 °C. The onset temperature (T_o), peak temperature (T_p), and conclusion temperature (T_c) are expressed in degrees Celsius. The enthalpy of gelatinisation (ΔH) is expressed in Joules per g (J/g). Because of the complete absence of amylose for the EH6 waxy mutant, no amylose−lipids dissociation data could be obtained. Results displayed are the means of three independent assays.

DP < 30), Baxter, Westonia, and Pastor had the highest percentage, and Xiaoyan54, AC-Barrie, and Chara had the lowest. Concerning the very long chains DP > 30, Westonia and Alsen displayed the highest percentage, and Pastor and Xiaoyan54 displayed the lowest.

Starch Gelatinization Properties. To investigate associations between structural and visco-properties, the swelling and gelatinization properties of the selected starches have been established. The starches displayed varying levels of swelling index (SI) (**Table 2**), ranging between 11.15 and 15.91. The two control lines (EH6 and Yamamori) displayed a very atypical SI due to their particular phenotypes. Except for these two controls, Alsen displayed the highest SI. The starches were also analyzed by DSC after water addition and equilibration described by Konik-Rose et al. (*22*). All of the genotypes displayed the same profile with onset (T_o), peak (T_p), and conclusion (T_c) temperature on average of 61, 64, and 70.5 °C, respectively. The gelatinization enthalpies (ΔH) determined by DSC may be related to their crystallinity (*28*). In our study, Chara demonstrated the highest enthalpy (5.90), and AC-Barrie demonstrated the lowest (4.81).

Lipids are associated with amylose in native starch granules. Swelling and gelatinization properties might be different if amylose is associated with lipids or are lipid-free. During DSC analysis and in particular gelatinization, amylose−lipid complexes crystallize. With further heating during the DSC process, lipids dissociate from amylose. This is seen as a peak around 90−130 °C. In our study, Xiaoyan54 displayed the highest enthalpy of amylose−lipid dissociation.

Starch Pasting Properties. RVA was used to investigate the starch pasting properties of these various genotypes. Profiles for six selected genotypes are illustrated in **Figure 4**. The five remaining RVA profiles (including VolcaniDD1, Pastor, Westonia, Yipti, and Baxter) are like the Chara profile and have not been shown for more clarity. However, **Table 3** displays the complete RVA characteristics including pasting temperature (temperature of first detectable viscosity), viscosity peak, breakdown, final viscosity, hot paste, and setback. The pasting temperatures of the genotypes were very similar (around 65 °C) with the notable exception of AC-Barrie and Xiaoyan54 (76.45 and 78.95 °C, respectively).

On the basis of their particular pasting properties (peak viscosity, hot paste, and final viscosity), we classified the samples into three groups: (i) high pasting properties group including Baxter, Chara, and Xiaoyan54 (displaying high peak, hot paste, and final viscosity); (ii) intermediate pasting property group including Yitpi, VolcaniDD1, Pastor, AC-Barrie, and Westonia (displaying high/average peak viscosity but average hot paste and/or final viscosity); and a low pasting property genotype, Alsen (average peak, low hot paste, and low final viscosity). Because of its particular phenotype and composition, the RVA profile from Yamamori is close to the detection level

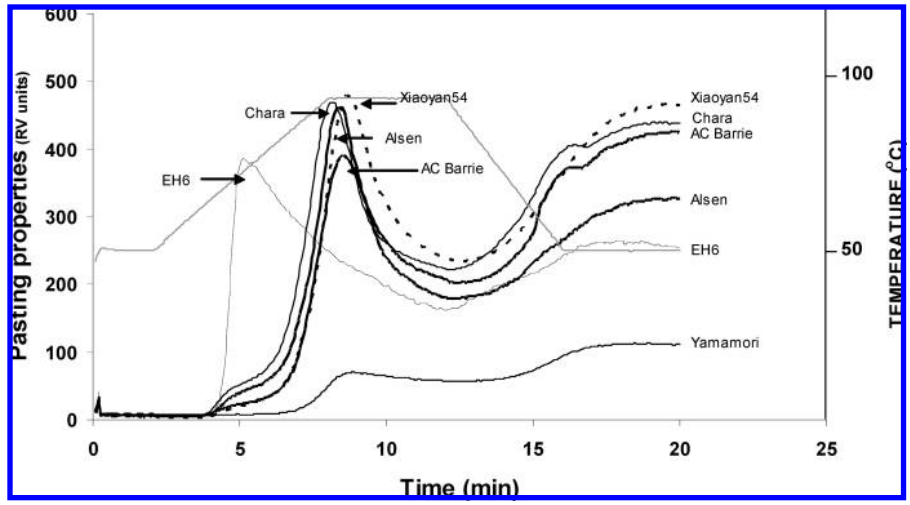

Figure 4. RVA profiles from various wheat genotypes. Six main RVA pasting curves of several wheat flours have been displayed. Thhe temperature profile is depicted in gray.

Table 3. Pasting Properties of Wheat Starches[a]

		viscosity (RVU)					
	pasting temp	peak	peak time	hot paste	breakdown	final viscosity	setback
Yamamori	87.4	58.67	8.87	47	11.67	93	46
EH6	65.55	322.75	5.13	134.42	188.33	211.17	76.75
VolcaniDD1	66.45	380.83	8.6	175.25	205.58	334.83	159.58
Pastor	66.05	403.58	8.33	163.25	240.33	313.33	150.08
AC-Barrie	76.45	325.33	8.53	168.5	156.83	355.33	186.83
Alsen	65.4	385.25	8.4	149	236.25	271.83	122.83
Westonia	64.95	418.67	8.33	176.5	242.17	339.83	163.33
Xiaoyan54	78.95	399.25	8.67	195.08	204.17	387.92	192.83
Yipti	65.55	405.33	8.27	166.75	238.58	325.33	158.58
Chara	63.5	390.92	8.07	184.5	206.42	366.08	181.58
Baxter	65.4	382.33	8.4	182.92	199.42	370	187.08

[a] Pasting temperatures are expressed in degrees Celsius. Viscosity properties are expressed in RVU. Results displayed are the means of three independent assays.

of the current calibration. It required special calibration, we did not consider it in the statistical analysis, and it was unrealistic to classify it into one of these groups.

PCA. To assess relationships between structural, molecular, and gelatinization properties, we aimed to identify a potential cause/effect relationship and a rapid screening method. First, a PCA has been performed. PCA takes complex correlated data arranged in a multidimensional space and reduces the data into a more simplified linearized axes while retaining as much of the original variation as possible. Correlated components form a correlation matrix, where the variances of the standardized data along an axis (eigen vectors) are the principal components. These axes correspond to the largest eigen values in the direction of the largest variation of the data.

The PCA revealed four principal components, which individually explained more than 10% of the variance and a combined total of 80% of the variance. The loadings and percent variance explained for each of the more relevant components are shown in **Table 4**. Plots of two of the four principal components can be seen in **Figure 5** with the dot positions indicating the relative importance of each of the loadings for each component. On the basis of the loading, each of the principal components may be subjectively grouped according structural, molecular, and gelatinization properties and their relationships.

The first principal component (PC1) related to the structural analysis of the starch is shown in **Figure 5**. The β-amylolysis shorter chains (Bam7 on the **Figure 5**) and the percent starch in flour (starch flour on the **Figure 5**) have positive loadings as do those for the gelatinization properties (DSC_Gel_To), indicating that these traits are positively related, and increasing the number of short internal chains may lead to an increase in the temperature of gelatinization initiation. In the same component (PC1), it could be seen that a number of traits were affected by changes to the structural and molecular components. Those with the largest loadings were RVA peak time and amylose−lipid dissociation properties (DSC_Aml_To and DSC_Aml_Tp), all with negative loadings associated with the percent amylose in the starch. Among the individual cultivars, Alsen and Chara showed the most extreme phenotypes described by PC1. This may be due to the differences in chain length distributions for both the isoamylase and the β-amylase chain lengths described above.

The second principal component appeared to be driven again by two more extreme phenotypes, Xiaoyan54 and again Alsen. There were three major features for this component. The first is the lipid content (Fatty Acid Starch^{-1}) and associated effects on peak time, pasting temperature (RVA peak Temp), and also final viscosity (RVA Final Visco). All were in the same relative direction (positive), which suggests a tight positive correlation between them. The second feature for this component was the chain length distribution and associated effects. Alsen had an atypical distribution for the chain length distribution, having a much larger percentage of short chain lengths along with an altered percentage of B-granules. The same loadings for the chain lengths (CL_10_11 and CL_12_14, respectively) had the same negative loading as starch SI (SI90c) and starch gelatinization (DSC_Gel_To), indicating a negative link between viscosity

Table 4. Correlation Analysis between Starch Pasting Properties and Structural Components[a]

	Bam_5	Bam_6	Bam_7	Bam_8	Bam_9	Bam_10	Bam11_12	Bam13_17	Bam18_23	CL_6_9	CL_10_11	CL_12_14	CL_15_17	CL_18_25	λmStarch
RVA Breakdown	0	−0.07	−0.12	0.12	−0.48	−0.37	−0.11	−0.03	0.27	0.31	0.32	0.22	−0.36	−0.31	−0.26
RVA Hot_paste	0.14	0.01	0.26	0	0.45	0.09	0.28	−0.15	−0.46	−0.6	−0.78*	−0.62	0.57	0.77*	0.26
RVA Visc_Peak	0.07	−0.07	0.01	0.13	−0.27	−0.34	0.02	−0.11	0.05	0.02	−0.06	−0.08	−0.08	0.07	−0.14
RVA Peak_Time	−0.74*	0.13	−0.67*	−0.52	0.19	0.47	0.2	0.74*	0.37	−0.34	0.06	0.19	−0.36	0.01	−0.63
RVA Setback	0.29	−0.01	0.42	0.17	0.47	0.02	0.07	−0.16	−0.4	−0.7*	−0.82**	−0.64	0.72*	0.81**	0.36
RVA peak_Temp	−0.22	0.19	−0.23	−0.18	0.26	0.09	0.01	0.28	−0.11	−0.48	−0.21	−0.14	−0.01	0.3	−0.49
RVA Final_Visc	0.24	0	0.37	0.11	0.48	0.05	0.15	−0.16	−0.44	−0.69*	−0.84**	−0.65	0.69*	0.82**	0.33
Swel. index	0.21	−0.01	−0.06	0.3	−0.52	−0.45	−0.43	−0.29	0.07	0.58	0.65	0.38	−0.66	−0.61	−0.44
DSC_AmL_ΔH	−0.22	0.19	−0.29	−0.22	−0.07	−0.35	0.37	0.11	−0.09	0.2	0.24	0.33	−0.32	−0.19	−0.35
DSC_AmL_Tc	−0.08	−0.02	−0.08	−0.03	−0.24	0.3	−0.18	0.05	0.32	0.34	0.34	0.2	−0.13	−0.39	0.27
DSC_AmL_To	−0.69*	0.2	−0.66	−0.32	−0.2	0.3	−0.09	0.82**	0.75*	−0.43	0.03	0.1	−0.29	0.04	−0.55
DSC_AmL_Tp	−0.41	0.08	−0.53	−0.29	−0.26	0.01	0	0.33	0.36	0.66	0.93**	0.85**	−0.82**	−0.89**	−0.54
DSC_gel_ΔH	0.57	0.03	0.43	0.31	−0.03	−0.52	0.02	−0.73*	−0.69*	0.27	−0.05	−0.17	0.1	0.04	0.16
DSC_gel_Tc	0.04	−0.29	0.14	−0.3	0.42	0.29	0.52	−0.25	−0.42	0.76*	0.46	0.49	−0.13	−0.53	0.35
DSC_gel_To	0.33	−0.2	0.45	−0.16	0.56	0.29	0.48	−0.57	−0.84**	0.3	−0.17	−0.19	0.41	0.08	0.6
DSC_gel_Tp	0.15	−0.25	0.3	−0.26	0.51	0.34	0.57	−0.37	−0.58	0.51	0.08	0.14	0.21	−0.18	0.61

	Am.Flour^{-1} (%)	Am.Starch^{-1} (%)	Starch.flour^{-1} (%)	AveGranuleSize	B-gran %	Glc6P	Prot_content	Behenic	Lignoceric	cis_11_Eicosenoic	FatAcid.Starch^{-1} (%)
RVA Breakdown	−0.37	−0.31	−0.16	0.38	−0.21	−0.18	−0.05	0.03	−0.61	−0.54	−0.05
RVA Hot_paste	−0.37	−0.36	0.09	0.28	−0.48	0.31	0.08	0.46	0.21	0.49	0.32
RVA Visc_Peak	−0.58	−0.51	−0.12	0.55	−0.47	−0.03	−0.01	0.27	−0.54	−0.31	0.11
RVA Peak_Time	0.28	0.49	−0.64	−0.02	−0.21	0.77*	0.32	0.64	0.74*	0.75*	0.46
RVA Setback	−0.12	−0.16	0.19	0.14	−0.34	0.28	−0.2	0.2	0.4	0.46	0.16
RVA peak_Temp	0.39	0.55	−0.44	−0.14	−0.21	0.74*	0.04	0.56	0.95**	0.72*	0.65
RVA Final_Visc	−0.22	−0.24	0.16	0.2	−0.41	0.3	−0.1	0.31	0.34	0.49	0.22
Swel. index	0	0.07	−0.21	−0.14	0.27	−0.14	−0.03	0.1	−0.17	−0.29	0.06
DSC_AmL_ΔH	0.18	0.33	−0.37	−0.08	−0.15	0.25	0.22	0.74*	0.09	0.36	0.7*
DSC_AmL_Tc	0.04	−0.08	0.24	−0.14	0.45	−0.47	0.01	−0.83**	−0.41	−0.54	−0.71*
DSC_AmL_To	0.12	0.3	−0.62	0.31	−0.34	0.61	−0.02	0.03	0.34	0.14	0.04
DSC_AmL_Tp	0.63	0.72*	−0.36	−0.53	0.53	0.01	0.22	0.16	0.2	0.1	0.17
DSC_gel_ΔH	−0.17	−0.2	0.23	−0.14	0.05	−0.24	0.04	0.26	−0.17	−0.03	0.34
DSC_gel_Tc	0.23	0.08	0.48	−0.63	0.64	−0.59	0.47	0.15	−0.21	0.15	−0.04
DSC_gel_To	−0.11	−0.31	0.68*	−0.37	0.31	−0.52	0.41	−0.03	−0.2	0.05	0.01
DSC_gel_Tp	−0.01	−0.21	0.63	−0.44	0.45	−0.61	0.45	0.01	−0.33	0.09	−0.11

[a] This analysis calculates the covariance of the data sets divided by the product of their standard deviations. For clarity, the table showed only the major results of the analysis. Significant correlations are highlighted in gray. Degrees of significance are indicated (* or **). The abbreviation footnote is the following: Bam_X, β-amylolysis chain with X glucose residues; CL_X_Y, chain length distribution from X to Y glucose residues; λmStarch, wavelength at the maximum absorbance for the complex iodine/polysaccharaide or λ_{max}; Am.Flour^{-1}(%), percentage of amylose in flour; Am.Starch^{-1} (%), percentage of amylose in starch; Starch.flour^{-1} (%), starch content in flour; AveGranuleSize, average starch granule size; B-gran %, percentage of B granule; Glc6P, glucose-6-phosphate content; Prot_content, starch protein content; Behenic, starch Behenic acid content; Lignoceric, starch lignoceric acid content; cis_11_Eicosenoic, starch *cis*11-eicosenoic acid content; FatAcid.Starch^{-1}, total starch fatty acid content; RVA Breakdown, RVA starch breakdown; RVA Hot_paste, RVA hot paste viscosity; RVA Visc_Peak, RVA peak viscosity; RVA Peak_Time, RVA peak time; RVA Setback, RVA setback: difference between final viscosity and hot paste; RVA peak_Temp, RVA pasting temperature; RVA Final_Visc, RVA final viscosity; Swel. Index, SI at 90 °C; DSC_AmL_ΔH, differential scanning calorimeter (DSC) amylose/lipid dissociation enthalpy; DSC_AmL_Tc, DSC amylose/lipid dissociation ending temperature; DSC_AmL_To, DSC amylose/lipid dissociation onset temperature; DSC_AmL_Tp, DSC amylose/lipid dissociation peak temperature; DSC_gel_ΔH, DSC starch gelatinization enthalpy; DSC_gel_Tc, DSC starch gelatinization ending temperature; DSC_gel_To, DSC starch gelatinization onset temperature; and DSC_gel_Tp, DSC starch gelatinization peak temperature.

traits and both the CE distribution and lipid content. In addition, the medium chain length (CL_15_17 and CL_18_25) conversely had a positive loading as final viscosity and suggests a close positive link between these factors. Finally, the third feature for this component was the Glc6P (G6P) and its close positive loading with RVA peak time and RVA pasting temperature (RVA peak temp). The grouping of Glc6P, RVA peak time, and RVA pasting temperature (all in the same relative, positive direction) in the PC analysis highlighted the potential value of using this assay as a screening method for wheat selection. The Glc6P is also loaded in the opposite direction of the SI (SI90c) for PC2.

The third and fourth principal components are less easily interpreted from a biological point of view. However, the *cis*-11-eicosenoid acid content shows a high loading in the same direction as that of the amylose−lipid dissociation enthalpy, whereas the remaining lipid traits are associated with the fourth component and the DSC enthalpies for amylose (data not shown).

Statistical Correlation between Molecular Characteristic and Pasting Properties. Previous studies have demonstrated a role of the amylose fraction on viscosity and use this trait as a marker of viscosity (*3, 29*). From PC2, we found an opposing loading between amylose content and some pasting traits like hot paste and final viscosity. We also found correlations among all of the amylose−lipid dissociation characteristics that we obtained via the DSC. There is no doubt that amylose affects wheat starch visco-properties. However, the number of convincing correlations with amylose content was below expectation. Batey et al. (*30*) suggested that, over 22% amylose, the flour quality for viscous products decreased. This optimum may explain why we did not establish higher correlations. Another hypothesis would be that it is not only the amylose content that affects the viscosity but also the alteration of the amylopectin structure. A recent study in *C. reinhardtii* suggests the involvement of the Granule Bound Starch Synthase (GBSSI) in the amylose production via the synthesis of very long chains of amylopectin (*31*). The tight interaction between amylose production and amylopectin structure may explain why we could have a strong effect from the amylose content on pasting properties without any strong correlation in our study.

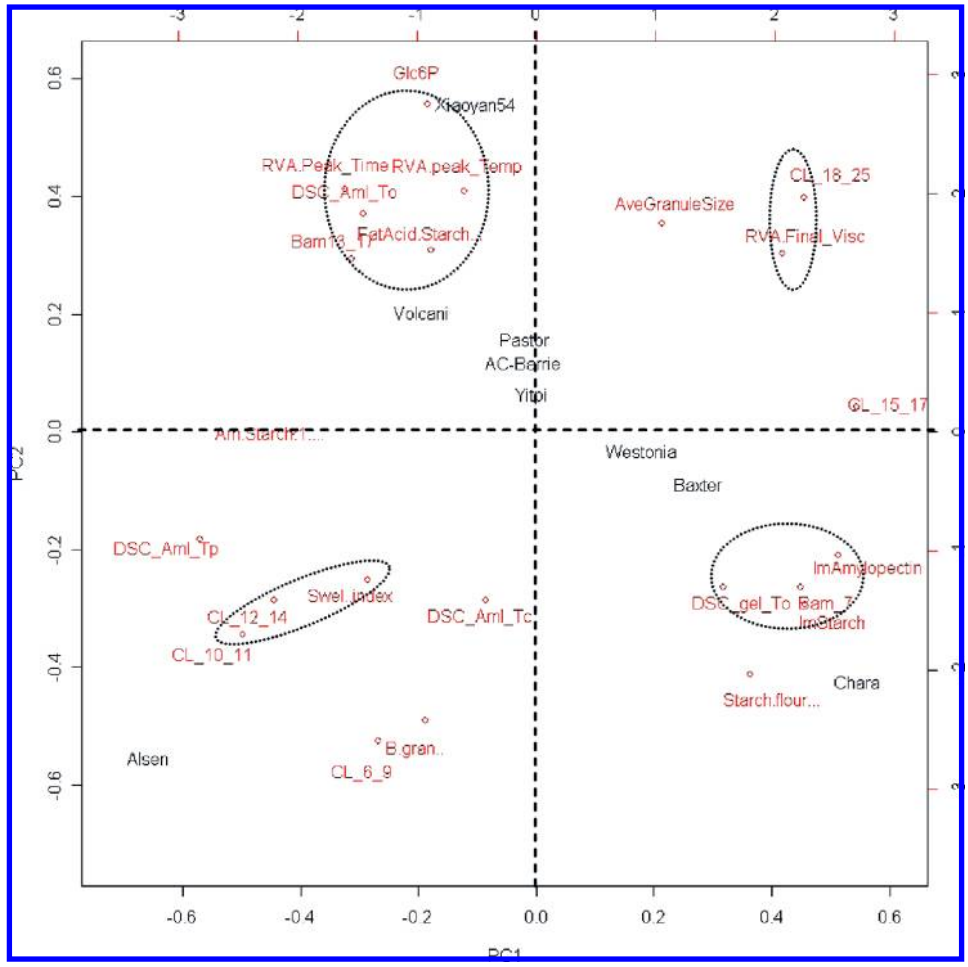

Figure 5. Principal component analyses. Loadings and percent variance explained for each of the components are shown in this figure. Plots of two of the four principal components can be seen with the dot position indicating the relative importance of each of the loadings for each component. For clarity, the figure showed only the major results of the analysis. The abbreviations used are similar to that used in **Table 4**.

Amylopectin short chains (CL_6−11) were negatively correlated to the RVA final viscosity (−0.84), hot paste (−0.78), and setback (−0.82) and positively correlated to the gelatinization T_c (0.76). However, glucan chains longer than 16 glucose residues were positively correlated to the RVA final viscosity (0.82), hot paste (0.78), and setback (0.81) and negatively correlated to the gelatinization T_c (−0.89). In addition, in the PCA, the medium chain length (CL_18−25) was more closely associated with final viscosity. The β-limit dextrin analysis also had a higher correlation with viscosity properties. β-Limit short chain lengths of five and seven seemed to affect the peak time. We also observed a negative correlation between intermediate β-limit chains (up to 18 glucose residues) and these gelatinization properties.

Shorts chains are known to be located on the external part of the crystalline structure (*32*). Because of their lengths, short chains cannot form stable double helical structures. Therefore, they are likely to be easily disrupted by the heat. It is logical to find a strong correlation between the short chains and the swelling properties of the starch granule. Conversely, the work of Sang-Ho and Jay-Lin (*29*) on wheat and Albert et al. (*10*) on cassava revealed the importance of long chains of amylopectin on pasting properties. They suggested that a higher proportion of longer chains (DP > 67) could be associated with amylose chain lengths forming longer helical structures and giving high gelatinization gel properties. Yamin et al. (*33*) suggested that these double helical structures require a higher temperature to dissociate than shorter double helices. The negative correlations that we found for the amylopectin long chain with viscosity are in agreement with this.

Despite the correlations established with the chains length distribution, the capillary electrophoresis method does not represent a high throughput protocol for screening large populations. However, the chain lengths with the same loadings on the PC analysis as the percent amylose in starch and flour were those between 10−14, and those chain lengths between 15−17 were associated with λ_{max} amylopectin. λ_{max} was also in the opposite direction to that of the pasting peak temperature along with RVA pasting peak time. This highlights the usefulness of λ_{max} as a screening method not only for altered chain length distributions, but it may be a useful screen for starch pasting properties.

No strong correlations were found with major fatty acids present in majority in the starch granule (data not shown). However, the pasting temperature was positively correlated to lignoceric acid (0.95) and eicosenoic acid (0.72). In addition, the peak time also displayed a positive correlation with these fatty acids (0.74 and 0.75, respectively). We also found behenic and the 11-eicosenoic acids were also correlated to the amylose dissociation properties obtained by DSC. Despite their low amounts in wheat (around 1% of the granular weight), Morrison et al. (*7*) have reported that internal lipids affect the swelling of starch, but no further determinants have been identified in wheat. The importance of minor fatty acids in viscosity has already been demonstrated in corn and potato starch. Raphaelides

and Georgiadis (*34*) altered maize starch viscosity by adding minor fatty acids into starch preparation.

Significant correlations have been found with peak time and pasting temperature, suggesting the role of monoesterified phosphate groups in the pasting properties. The presence of phosphate groups in starch may affect the water absorption capacity of starch pastes after gelatinization (*14*). The negative charges present in the monoesterified phosphate may generate repulsion between the chains. These chains would be more likely able to interact with water molecules and, therefore, display weakness to high temperature. The common explanation for the differences in viscosity between potato and cereal is their phosphate content. Starch from potato tuber displays an average of 25 nmol of Glc6P per mg starch while cereal starches display 10 times less Glc6Ps in their reserve starch (*35*). However, it is interesting to see that, even with a very low amount, monoesterified phosphate groups may still have an influence on pasting or visco-properties of wheat starch. Further developments need to be realized to confirm and validate this hypothesis.

This study highlights some potential cause/effect relationships between molecular and structural traits and viscosity properties. Molecular factors such as starch lipids and monoesterified phosphate seem to be related to the initiation of the starch swelling processes (pasting temperature and peak time). External short chains may also be related to peak time and seem to be part of the early swelling process. However, the main structure of amylopectin (revealed by the chain length distribution analysis) is clearly related to the late process of starch swelling (including hot paste and final viscosity). Finally, no cause/effects relationships were highlighted for the first viscosity peak. This could be more likely due to a complex association of various parameters for which no individual parameter could be associated given the sample size.

A number of key parameters have been identified in this study that could be used in prebreeding/breeding programs to tailor wheat starch properties. We highlight the association between particular chain lengths and the starch visco-properties, not only amylose but also the involvement of amylopectin chains. We also suggest via the PCA that measuring λ_{max} could represent a high throughput method for screening large populations to detect genotypes with particular structures and therefore particular viscosities. In this case, the implications of Glc6P in both of the pasting properties constitute another good screening method to characterize wheat genotypes for viscosity traits.

Despite their low amount, this study also demonstrates the implication of internal fatty acids in pasting properties, in particular lignoceric acid. Wheat starch granules are known to contain more lipids than potato starch (*36*). The relatively low content of relevant lipids in relation to viscosity could represent a new potential in terms of wheat starch viscosity. Altering this fatty acid metabolism may have an interesting impact on wheat starch viscosity.

The potential of these correlations has to be confirmed across a larger data set. The screening of a large wheat mapping population will be undertaken to validate the result as well as to define genetic markers for wheat starch viscosity.

ACKNOWLEDGMENT

We acknowledge Sadequr Rahman and Zhongyi Li for the scientific support provided at various stages of the inception and execution of this work, Jeni Pritchard for technical assistance, Dick Philips for mass spectrometry, and Loraine Mason for lipids analysis.

LITERATURE CITED

(1) Buléon, A.; Colonna, P.; Planchot, V.; Ball, S. Starch granules: Structure and biosynthesis. *Int. J. Biol. Macromol.* **1998**, *23*, 85–112.
(2) Rask, O. S.; Alsberg, C. L. A viscosimetric study of wheat starches. *Cereal Chem.* **1924**, *1*, 7–26.
(3) Zeng, M.; Morris, C. F.; Batey, I. L.; Wrigley, C. W. Sources of variation for starch gelatinization, pasting, and gelation properties in wheat. *Cereal Chem.* **1997**, *74*, 63–71.
(4) Oda, M.; Yasuda, Y.; Okazaki, S.; Yamauchi, Y.; Yokoyama, Y. A method of flour quality assessment for Japanese noodles. *Cereal Chem.* **1980**, *57*, 253–254.
(5) Cooke, D.; Gidley, M. J. Loss of crystalline and molecular order during starch gelatinization and origin of the enthalpic transition. *Carbohydr. Res.* **1992**, *227*, 103–112.
(6) Galliard, T.; Bowler, P. Morphology and composition of starch. In *Critical Reports on Applied Chemistry, Starch: Properties and Potential*; Galliard, T., Ed.; J. Wiley and Sons: Great Britain, 1987; Vol. 13, pp 57−78.
(7) Morrison, W. R.; Tester, R. F.; Snape, C. E.; Law, R.; Gidley, M. J. Swelling and gelatinization of cereal starches. IV. Some effect of lipid-complexed amylose and free amylose in waxy and normal barley starches. *Cereal Chem.* **1993**, *70*, 385–389.
(8) Zhang, G.; Venkatachalam, M.; Hamaker, B. R. Structural basis for the slow digestion property of native cereal starches. *Biomacromolecules* **2006**, *7* (11), 3259–3266.
(9) Madsen, M. H.; Christensen, D. H. Changes in viscosity properties of potato starch during growth. *Starch/Stärke* **1995**, *48*, 76–79.
(10) Albert, L. C.; Yung, H. C.; Wen, C. K.; Klanaroth, S.; Tzou, C. H. Influence of amylopectin and amylose content on the gelling properties of five cultivars of Cassava starches. *J. Sci. Food Agric.* **2005**, *53*, 2717–2725.
(11) Evans, I. D.; Haisman, D. R. Rheology of gelatinized starch suspensions. *J. Texture Stud.* **1979**, *17*, 253–257.
(12) Kim, S. Y.; Wiesenborn, D. P.; Orr, P. H.; Grant, L. A. Screening potato starch for novel properties using differential scanning calorimetry. *J. Food Sci.* **1995**, *60*, 1060–1065.
(13) Lii, C. Y.; Tsai, M. L.; Tseng, K. H. Effect of Amylose content on the rheological property of rice starch. *Cereal Chem.* **1996**, *73*, 415–420.
(14) Singh, N.; Singh, J.; Kaur, L.; Singh Soghi, N.; Singh Gill, B. Morphological, thermal and rheological properties of starches from different botanical sources. *Food Chem.* **2003**, *81*, 219–231.
(15) Akbari, R. Development Core Team. In *A Language and Environment for Statistical Computing*; R Foundation for Statistical Computing: Vienna, Austria, 2006; ISBN 3-900051-07-09.
(16) Lii, C. Y.; Lineback, D. R. Characterisation and comparison of cereal starches. *Cereal Chem.* **1977**, *54*, 138–149.
(17) Konik-Rose, C. M.; Moss, R.; Rahman, S.; Appels, R.; Stoddard, F. L.; McMaster, G. Evaluation of the 40 mg swelling test for measuring starch functionality. *Starch/Stärke* **2001**, *53*, 14–20.
(18) Konik, C. M. Differential scanning calorimetry of wheat starch. *Proc. 45th Aust. RACI Cereal Chem. Conf.* **1995**, 140–144.
(19) Eliasson, A.-C.; Karlsson, K. Gelatinisation properties of different size classes of wheat starch granules measured by differential scanning calorimeter. *Starch/Stärke* **1983**, *35*, 130–133.
(20) Mohammadkhani, A.; Stoddard, F. L.; Marshall, D. R. Survey of amylose content in *Secale cereale Triticum monococcum*, *T. turgidum* and *T. tauschii*. *J. Cereal Sci.* **1998**, *28*, 273–280.
(21) Morell, M. K.; Samuel, M. S.; O'Shea, M. G. Analysis of starch structure using fluorophore-assisted carbohydrate electrophoresis. *Electrophoresis* **1998**, *19*, 2603–2611.
(22) Azudin, M. N.; Morrison, W. R. Variation in the amylose and lipid contents and some physical properties of rice starches. *J. Cereal Sci.* **1986**, *5*, 35–37.
(23) Morrison, W. R.; Milligan, T. P.; Azudin, M. N. A relationship between the amylose and lipid contents of starches from diploid cereals. *J. Cereal Sci.* **1984**, *2*, 257–271.
(24) Ekman, P.; Jager, O. Quantification of subnanomolar amounts of phosphate bound seryl and theronyl residues in phosphoproteins

using alkaline hydrolysis and malachite green. *Anal. Biochem.* **1993**, *214*, 138–141.
(25) Blennow, A.; Bay-Smidt, A. M.; Wischmann, B.; Olsen, C. E.; Møller, B. L. The degree of starch phosphorylation is related to the chain length distribution of the neutral and the phosphorylated chains of amylopectin. *Carbohydr. Res.* **1998**, *307*, 45–54.
(26) Davies, T. G. E.; Ying, J.; Xu, Q.; Li, Z. S.; Li, J.; Gordon-Weeks, R. Expression analysis of putative high-affinity phosphate transporters in Chinese winter wheats. *Plant Cell Environ.* **2002**, *25* (10), 1325–1339.
(27) Banks, W.; Greenwood, C. T.; Muir, D. D. The characterisation of starch and its components. Part 3. The techniques of semi-micro, differential, potentiometric iodine titration and the factors affecting it. *Starch/Stärke* **1971**, *23*, 118–124.
(28) Krueger, B. R.; Knutson, C. A.; Inglett, G. E.; Walker, C. E. A differential scanning calorimetry study on the effect of annealing on gelatinization behavior of corn starch. *J. Food Sci.* **1987**, *52*, 715–718.
(29) Sang-Ho, Y.; Jay-Lin, J. Structural and physical characteristics of waxy and other wheat starches. *Carbohydr. Polym.* **2002**, *49*, 297–305.
(30) Batey, I. L.; Gras, P. W.; Curtin, B. M. Contribution of the chemical structure of wheat starch to Japanese noodle quality. *J. Sci. Food Agric.* **1997**, *74*, 503–508.
(31) Ral, J.-P.; Colleoni, C.; Wattebled, F.; Dauvillee, D.; Nempont, C.; Deschamps, P.; Li, Z. Y.; Morell, M. K.; Chibbar, R.; Purton, S.; d'Hulst, C.; Ball, S. G. Circadian clock regulation of starch metabolism establishes GBSSI as a major contributor to amylopectin synthesis in *Chlamydomonas reinhardtii*. *Plant Physiol.* **2006**, *142*, 305–317.
(32) Hizukkuri, S. Polymodal distribution of the chain lengths of amylopectins and its significance. *Carbohydr. Res.* **1986**, *147*, 342–347.
(33) Yamin, F. F.; Lee, M.; Pollk, L. M.; White, P. J. Thermal properties of starch in corn variants isolated after chemical mutagenesis of inbred line B73. *Cereal Chem.* **1999**, *76*, 175–181.
(34) Raphaelides, S. N.; Georgiadis, N. Effect of fatty acids on the rheological behaviour of maize starch dispersions during heating. *Carbohydr. Polym.* **2006**, *65*, 81–92.
(35) Blennow, A.; Wischmann, B.; Houborg, K.; Ahmt, T.; Jorgensen, K.; Engelsen, S. B.; Bandsholm, O.; Poulsen, P. Structure function relationships of transgenic starches with engineered phosphate substitution and starch branching. *Int. J. Biol. Macromol.* **2005**, *36* (3), 159–168.
(36) Galliard, T. Starch availability and utilization. In *Critical Reports on Applied Chemistry; Starch: Properties and Potential*; Galliard, T., Ed.; J. Wiley and Sons: Great Britain, 1987; Vol. 13, pp 1−15.

Received for review January 14, 2008. Revised manuscript received March 6, 2008. Accepted March 17, 2008. We also acknowledge the financial support provided by GRDC for this work.

JF800124F